

UNCLASSIFIED

**Defense Technical Information Center
Compilation Part Notice**

ADP014825

TITLE: MHD Turbulence at Moderate Magnetic Raynolds Number

DISTRIBUTION: Approved for public release, distribution unlimited

This paper is part of the following report:

TITLE: Annual Research Briefs - 2003 [Center for Turbulence Research]

To order the complete compilation report, use: ADA420749

The component part is provided here to allow users access to individually authored sections of proceedings, annals, symposia, etc. However, the component should be considered within the context of the overall compilation report and not as a stand-alone technical report.

The following component part numbers comprise the compilation report:

ADP014788 thru ADP014827

UNCLASSIFIED

MHD turbulence at moderate magnetic Reynolds number

By B. Knaepen, S. Kassinos† AND D. Carati‡

1. Introduction

1.1. Motivation and objectives

Magnetohydrodynamics applies to many conductive fluid and plasma flows encountered in nature and in industrial applications. In numerous circumstances, the flow is subject to a strong mean magnetic field. This happens in the earth's liquid core and is ubiquitous in solar physics for topics like sunspots, solar flares, solar corona, solar wind etc. Mean magnetic fields play an important role on even larger scales, for instance in the dynamics of the interstellar medium. Among the industrial applications involving applied external magnetic fields are drag reduction in duct flows, design of efficient coolant blankets in tokamak fusion reactors, control of turbulence of immersed jets in the steel casting process and advanced propulsion and flow control schemes for hypersonic vehicles.

Depending on the application, the magnetic Reynolds number, R_m , can vary tremendously. In astrophysical problems, R_m can be extremely high as a result of the dimensions of the objects studied. On the contrary, for most industrial flows involving liquid metal, R_m is very low, usually less than 10^{-2} . When an external magnetic field is present, it is customary at such low values of R_m to make use of the so-called quasi-static (QS) approximation. In this approximation, induced magnetic fluctuations are much smaller than the applied magnetic field and the overall magnetic effect amounts to adding in the Navier-Stokes equations an extra damping term which only affects Fourier modes having a component parallel to the magnetic field (more details below). The derivation of the QS approximation involves taking the limit of vanishing R_m and its domain of validity is thus an interesting question. Indeed certain applications, such as advanced schemes for the control of magnetogasdynamic flows around hypersonic vehicles, involve values of R_m of the order 1 to 10. It is thus valuable to possess reliable approximations in this regime that can be used in place of the full non-linear MHD.

The limit of vanishing R_m (with mean magnetic field) has been the subject of several theoretical studies in the past. In Lehnert (1955) the author concentrates on the final period of decay of a convective fluid governed by the completely linearized MHD equations ($Re \ll 1$, $R_m \ll 1$). The suppression of turbulence by a magnetic field was studied in Moffatt (1967) ($Re \gg 1$, $R_m \ll 1$) again using linearized equations. In short, both works focus on the time evolution of the energy of the Fourier modes as a function of their wave vectors. Using prescribed energy spectra, Moffatt (1967) also obtains global energy decay rates. Another theoretical investigation relevant to the present study is the work of Davidson (1995). In that article, the author derives in the quasi-static framework the conservation of momentum and angular momentum parallel to the direction of the

† Department of Mechanical and Manufacturing Engineering, University of Cyprus, 75 Kallipoleos, Nicosia 1678, Cyprus

‡ Université Libre de Bruxelles, Statistical and Plasma Physics, CP231, Boulevard du Triomphe, Campus Plaine, 1050 Brussels, Belgium.

magnetic field (neglecting viscous dissipation). Focusing on jets and vortices, the author then describes how the flow structures need to elongate in the direction of the magnetic field in order to lower their energy loss while satisfying the above conservation laws. The elongation of structures in the direction of the magnetic field was also studied earlier in Sommeria & Moreau (1982) however in the context of linearized equations.

To our knowledge, the first numerical study of MHD turbulence in the regime $R_m \ll 1$ is due to Schumann (1976). All the simulations in that work were done using a modified 3D spectral code implementing the QS approximation. However, due to the computer resources available at that time, the resolution of the simulations was limited to 32^3 . The numerical experiment of Schumann (1976) reproduces the thought experiment described in Moffatt (1967) in which an initially homogeneous isotropic flow is suddenly subjected to an applied external magnetic field. A quantitative description of the magnetic damping and building of anisotropy is presented as well as the dependence of the results on the presence or not of the non-linear term in the Navier-Stokes equation. Again considering the QS approximation, the case of forced turbulence in a 3D periodic domain has first been studied in Hossain (1991) and more recently in Zikanov & Thess (1998).

Performing FMHD simulations in the limit of low R_m is impractical. Aside from the increased complexity arising from having to carry a separate evolution equation for the magnetic field, the main problem lies in the time-scales involved in the problem. Indeed at vanishing magnetic Reynolds number, the magnetic diffusion time-scale tends to zero. The only possibility in that case is to resort to the QS approximation for which this time-scale is not explicitly relevant. Simulations of FMHD have thus been restricted so far to cases where the magnetic and kinetic time-scales are of the same order. This is the case when the magnetic Prandtl number (see below) is close to 1. Among the numerous previous numerical studies of MHD in this regime, we mention the work of Oughton *et al.* (1994) which is the most relevant to the present discussion. In that work, the authors consider the same 3D periodic geometry with an applied external magnetic field as in Schumann (1976).

In the present article we will consider the decay of MHD turbulence under the influence of a strong external magnetic field at moderate magnetic Reynolds numbers. Typical values of R_m that are considered here range from $R_m \sim 0.1$ to $R_m \sim 20$. As a comparison, the initial kinetic Reynolds number common to all our simulations is $Re_L = 199$. This means that the range of Prandtl numbers explored is 5×10^{-4} to 10^{-1} . Our motivation is mainly to exhibit how the transition from the QS approximation to FMHD occurs. At the lowest values of R_m studied here, the QS approximation is shown to model the flow faithfully. However, for the higher values of R_m considered, it is clearly inadequate but can be replaced by another approximation which will be referred to as the Quasi-Linear (QL) approximation. Another objective of the present study is to describe how variations in the magnetic Reynolds number (while maintaining all other parameters constant) affect the dynamics of the flow. This complements past studies where variations in either the strength of the external magnetic field or the kinetic Reynolds number were considered.

This article is organized as follows. In section 2 we recall the definition of the quasi-static approximation. Section 3 is devoted to the description of the numerical experiments performed using the quasi-static approximation and full MHD. In section 4 we describe the quasi-linear approximation and test it numerically against full MHD. A concluding summary is given in section 5.

2. MHD equations in the presence of a mean magnetic field

2.1. Dimensionless parameters

Two dimensionless parameters are usually introduced to characterize the effects of a uniform magnetic field applied to unstrained homogeneous turbulence in an electrically conductive fluid. They are the magnetic Reynolds number R_m and the interaction number N (also known as the Stuart number):

$$R_m \equiv \frac{vL}{\eta} = \left(\frac{L^2}{\eta} \right) / \left(\frac{L}{v} \right), \quad N \equiv \frac{\sigma B^2 L}{\rho v} = \frac{\tau}{\tau_m}. \quad (2.1)$$

In the above expressions, $v = \sqrt{\langle u_i u_i \rangle / 3}$ is the r.m.s. of the fluctuating velocity u_i ; L is the integral length scale of the flow; $\eta = 1/(\sigma\mu)$ is the magnetic diffusivity where σ is the electric conductivity of the fluid, and μ is the fluid magnetic permeability; ρ is the fluid density and B is the strength of the applied external magnetic field. The magnetic Reynolds number represents the ratio of the characteristic time scale for diffusion of the magnetic field L^2/η to the time scale of the turbulence $\tau = L/v$. Related to R_m , one can also define a magnetic Prandtl number representing the ratio of R_m to the hydrodynamic Reynolds number Re_L ,

$$P_m \equiv \frac{\nu}{\eta} = \frac{R_m}{Re_L}, \quad Re_L = \frac{vL}{\nu}. \quad (2.2)$$

The interaction number N represents the ratio of the large-eddy turnover time τ to the Joule time $\tau_m = \rho/(\sigma B^2)$, i.e. the characteristic time scale for dissipation of turbulent kinetic energy by the action of the Lorentz force (Davidson 2001). N can be viewed as a measure of the ability of an imposed magnetic field to drive the turbulence to a two-dimensional three-component state. Indeed, under the continuous action of the Lorentz force, energy becomes increasingly concentrated in modes independent of the coordinate direction aligned with \mathbf{B} . As a two-dimensional state is approached, Joule dissipation decreases because fewer and fewer modes with gradients in the direction of \mathbf{B} are left available. In addition, the tendency towards two-dimensionality and anisotropy is continuously opposed by non-linear angular energy transfer from modes perpendicular to \mathbf{B} to other modes, which tends to restore isotropy. If N is larger than some critical value N_c , the Lorentz force is able to drive the turbulence to a state of complete two-dimensionality. For smaller N , the Joule dissipation is balanced by non-linear transfer before complete two-dimensionality is reached. For very small N , the anisotropy induced by the Joule dissipation is negligible.

2.2. The Quasi-Static approximation

If the external magnetic field B_i^{ext} is explicitly separated from the fluctuations b_i , the MHD equations can be written as

$$\partial_t u_i = -\partial_i(p/\rho) - u_j \partial_j u_i + \frac{1}{(\mu\rho)} (B_j^{ext} + b_j) \partial_j (B_i^{ext} + b_i) + \nu \Delta u_i, \quad (2.3)$$

$$\partial_t (B_i^{ext} + b_i) = -u_j \partial_j (B_i^{ext} + b_i) + (B_j^{ext} + b_j) \partial_j u_i + \eta \Delta (B_i^{ext} + b_i), \quad (2.4)$$

where p is the sum of the kinematic and magnetic pressures and ν is the kinematic viscosity. Since we consider initially isotropic, freely decaying homogeneous turbulence there is no mean velocity field.

Also, the external magnetic field is taken to be homogeneous and stationary. Therefore,

Resolution	256^3
Box size ($l_x \times l_y \times l_z$)	$2\pi \times 2\pi \times 2\pi$
Rms velocity	1.76
Viscosity	0.006
Integral length-scale ($(3\pi/4 \times (\int \kappa^{-1} E(\kappa) d\kappa / \int E(\kappa) d\kappa))$)	0.679
$Re = uL/\nu$	199
Dissipation (ϵ)	8.39
Dissipation scale ($\gamma = (\nu^3/\epsilon)^{1/4}$)	0.0127
$k_{max}\gamma$	1.62
Microscale Reynolds number ($R_\lambda = \sqrt{15/(\nu\epsilon)}u^2$)	53.5
Eddy turnover time ($\tau = (3/2)u/\epsilon$)	0.554

TABLE 1. Turbulence characteristics of the initial velocity field. All quantities are in MKS units.

(2.3) and (2.4) reduce to

$$\partial_t u_i = -\partial_i(p/\rho) - u_j \partial_j u_i + \frac{1}{(\mu\rho)} b_j \partial_j b_i + \frac{1}{(\mu\rho)} B_j^{ext} \partial_j b_i + \nu \Delta u_i, \quad (2.5)$$

$$\partial_t b_i = -u_j \partial_j b_i + b_j \partial_j u_i + B_j^{ext} \partial_j u_i + \eta \Delta b_i. \quad (2.6)$$

As pointed out in Roberts (1967), this system can be simplified considerably for flows at low magnetic Reynolds numbers. Using a Fourier representation for u_i one has in this limit,

$$\partial_t u_m(\mathbf{k}, t) = -ik_m p'(\mathbf{k}, t) - [u_j \partial_j u_i]_m(\mathbf{k}, t) - \sigma \frac{(\mathbf{B}^{ext} \cdot \mathbf{k})^2}{\rho k^2} u_m(\mathbf{k}, t) - \nu k^2 u_m(\mathbf{k}, t), \quad (2.7)$$

where $p' = p/\rho$ and $u_m(\mathbf{k}, t) = \sum u_m(\mathbf{x}, t) e^{-i\mathbf{k} \cdot \mathbf{x}}$. Thus one can take into account the effect of the magnetic on the velocity field through a damping term and not solve explicitly the evolution equation for the magnetic fluctuations.

In the next sections, we test the QS approximation by comparing its predictions to those obtained using the full MHD equations (2.5) and (2.6).

3. Numerical Results: QS vs. FMHD

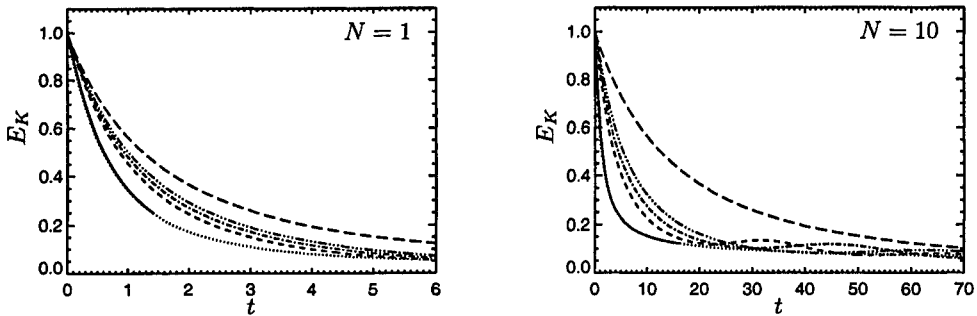
3.1. Parameters

To test the domain of validity of the QS approximation, we have used two different pseudo-spectral codes. The first one simulates the full MHD equations (2.5) and (2.6), while the second one simulates (2.7). All the runs presented here have a resolution of 256^3 Fourier modes in a $(2\pi)^3$ computational domain.

The initial condition for the velocity field is common to both codes. It consists of a developed turbulence field that is adequately resolved in the computational domain adopted. Some of its characteristics are listed in table 1. For the full MHD case, an initial condition for b_i has to be chosen at $t = t_0$. Here we have made the choice $b_i(t_0) = 0$. In other words, our simulations describe the response of an initially non-magnetized turbulent conductive fluid to the application of a strong magnetic field. The corresponding completely-linearized problem has been described in detail in Moffatt (1967). For the QS

#	η	B_A^{ext}	$N(t_0)$	$R_m(t_0)$
1	11.95	5.57	1	0.1
2	0.239	0.787	1	5.0
3	0.119	.557	1	10.0
4	0.0597	0.394	1	20.0
5	11.95	17.6	10	0.1
6	0.239	2.49	10	5.0
7	0.119	1.76	10	10.0
8	0.0597	1.24	10	20.0

TABLE 2. Summary of the parameters for the different runs performed

FIGURE 1. Evolution with time of the kinetic energy at different Stuart numbers and magnetic Reynolds numbers. QS approximation; —— $R_m = 0.1$; ----- $R_m = 5$; -·- ·- $R_m = 10$; -··- $R_m = 20$; - - - $B_A^{ext} = 0$.

approximation case, an initial condition for b_i is of course not required since the equation for the velocity field is completely closed.

In order to distinguish between our numerical runs, we will vary the values of the interaction parameter and the magnetic Reynolds number (at $t = t_0$). When these two quantities are set, the only free parameters in the evolution equations (2.5), (2.6) and (2.7) are completely determined, i.e.:

$$B_A^{ext} = \frac{Nv^2}{R_m}, \quad \eta = \frac{vL}{R_m}, \quad (3.1)$$

where B_A^{ext} is the external magnetic field strength in Alfvén units $B_A^{ext} = B^{ext}/\sqrt{\mu\rho}$ and the values of v and L are listed in table 1. The values of R_m and N for all our runs are listed in table 2 along with the corresponding values of η and B_A^{ext} .

3.2. Results

In this section we present some results obtained by performing the simulations detailed in section 3.1.

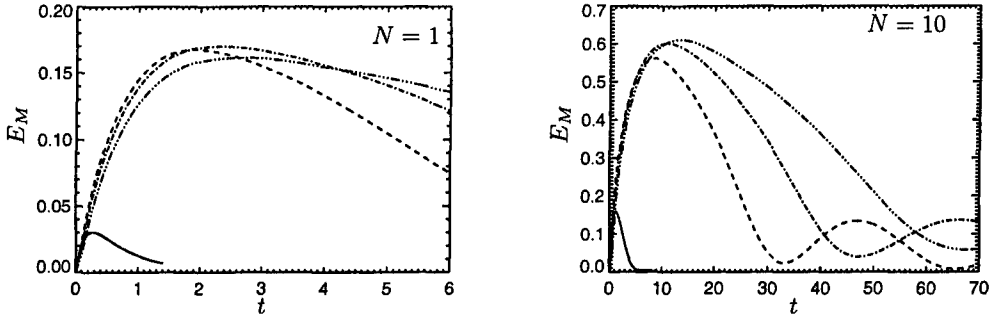


FIGURE 2. Evolution with time of the magnetic energy computed from (3.3). — $R_m = 0.1$;
- - - $R_m = 5$; - · - $R_m = 10$; - · - · - $R_m = 20$

3.2.1. Kinetic energy decay

In fig. 1 we plot the time evolution of the normalized kinetic energy,

$$E_K = \frac{1}{E_K(0)} \int d\mathbf{x} \frac{1}{2} u_i(\mathbf{x}) u_i(\mathbf{x}). \quad (3.2)$$

In this and subsequent figures, time has been non-dimensionalized using the Joule time-scale. Keeping N constant, it is clear from the figure that as the magnetic Reynolds number is decreased, the decays converge to the quasi-static limit (dotted curve). At $R_m = 0.1$, FMHD and the QS approximation are barely distinguishable for the cases run. As expected, the discrepancy between FMHD and the QS approximation is quite severe at intermediate values of the R_m . We also note here the presence of oscillations in the kinetic energy at long times for the case $N = 10$. Their origin is well known (Lehnert 1955; Moffatt 1967) and result from the laminarization of the flow for long times. In that case the MHD equations (2.5) and (2.6) reduce to their linear versions and become (in Fourier space) a system of linear oscillators coupled through the external magnetic field. In both figures, the case $B^{ext} = 0$ has been included to emphasize the role of the magnetic field in the other runs.

3.2.2. Magnetic energy evolution

The next diagnostic we examine is the evolution of the energy contained in the magnetic fluctuations. This quantity is defined through,

$$E_M = \int d\mathbf{k} \frac{1}{2} |b_i(\mathbf{k}, t)|^2. \quad (3.3)$$

and its time evolution is presented in Fig. 2. After some time, the magnetic energies all reach their maximum value and then start to decrease. The rate of decay increases at lower magnetic Reynolds numbers since in the limit chosen, $\eta = vL/R_m$. Related to the oscillations in the kinetic energy we observe for $N = 10$ some oscillations in the magnetic energy at long times.

3.2.3. Anisotropy

A characteristic feature of MHD flows subject to a strong external magnetic field is the appearance of a strong anisotropy in the flow. In the QS approximation this is easily seen by observing that in eq. (2.7) only Fourier modes with wave vectors having a nonzero projection onto B_i^{ext} are affected by the extra Joule damping. In order to quantify the

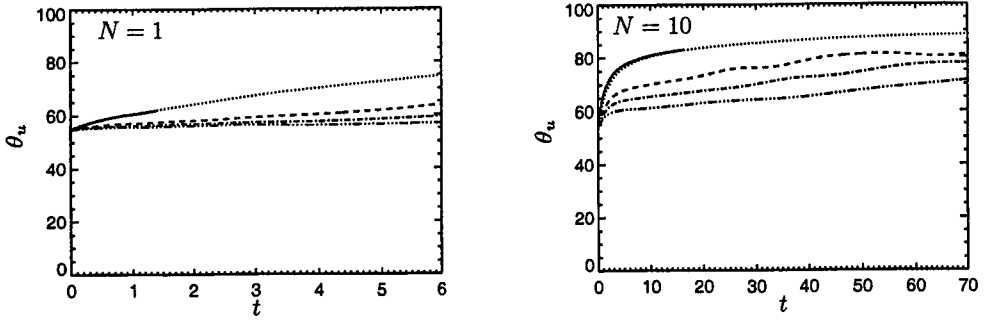


FIGURE 3. Anisotropy angle θ_u computed from (3.4). QS approximation; — $R_m = 0.1$; - - - $R_m = 5$; - · - $R_m = 10$; - · · - $R_m = 20$.

anisotropy we follow the approach of Shebalin *et al.* (1983) and Oughton *et al.* (1994) by introducing the anisotropy angles,

$$\tan^2 \theta_u = \frac{\sum k_\perp^2 \|u_i(\mathbf{k})\|^2}{\sum k_z^2 \|u_i(\mathbf{k})\|^2}, \quad (3.4)$$

$$\tan^2 \theta_b = \frac{\sum k_\perp^2 \|b_i(\mathbf{k})\|^2}{\sum k_z^2 \|b_i(\mathbf{k})\|^2}, \quad (3.5)$$

where $k_\perp = k_x^2 + k_y^2$ and the summations are extended to all values of \mathbf{k} .

When the flow is completely isotropic, one has $\tan^2 \theta_u = 2$ implying $\theta_u \simeq 54.7^\circ$. If the flow becomes independent of the z -direction then $\tan^2 \theta_u \rightarrow \infty$ or equivalently $\theta_u \rightarrow 90^\circ$. Figure 3 shows the evolution with time of θ_u for the different runs. At $N = 1$ the anisotropy is only important for the QS and $R_m = 0.1$ runs. For $N = 10$ all the runs become highly anisotropic.

The initial anisotropy in the magnetic field can also be computed exactly. At time $t_0 + \Delta t$ ($\Delta t \ll 1$), $b_i(\mathbf{k}, t_0 + \Delta t)$ is given by $b_i(\mathbf{k}, t_0 + \Delta t) = iB_z^{ext}k_z u_i(\mathbf{k}, t_0) \Delta t$. Using this form and the fact that u_i is initially homogeneous and isotropic one gets after some direct calculations,

$$\tan^2 \theta_b(t_0 + \Delta t) = \frac{2}{3}, \text{ i.e., } \theta_b(t_0 + \Delta t) \simeq 39.2^\circ. \quad (3.6)$$

Figure 4 shows the evolution with time of θ_b for the different runs. Both plots exhibit surprising behavior. In the case $N = 1$, one would expect θ_b to remain close to its initial value since the velocity field remains largely isotropic (as it is at the beginning of the simulation). Instead, θ_b evolves to a value compatible with an isotropic magnetic field. This is also the case for the runs at $N = 10$ although there the velocity field clearly evolves to an anisotropic state.

4. The Quasi-Linear approximation

4.1. Governing equations

The preceding section indicates that for our numerical simulations at magnetic Reynolds numbers of the order 10^{-1} the QS approximation and FMHD produce nearly identical results. For higher values of R_m the QS approximation is not valid and has to be replaced

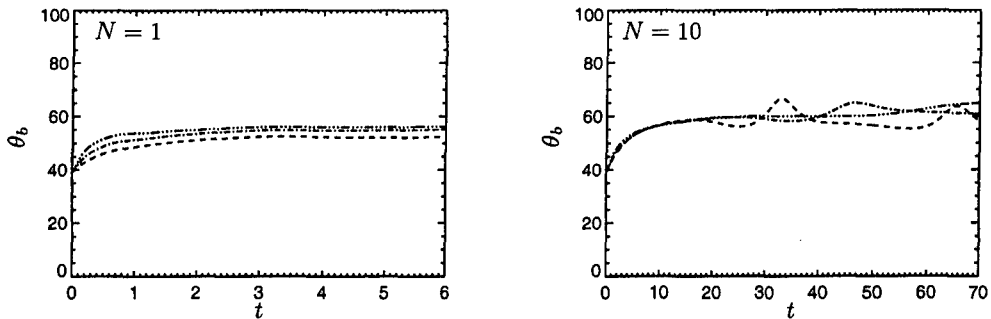


FIGURE 4. Anisotropy angle θ_b computed from (3.5). QS approximation; — $R_m = 0.1$; - - - $R_m = 5$; - - - $R_m = 10$; - - - - $R_m = 20$.

to predict the flow accurately. Since magnetic fluctuations remain small in all the runs performed, it is natural to still consider a linearized induction equation. We thus consider here an intermediate approximation which is defined by the following simplified MHD equations:

$$\partial_t u_i = -\partial_i(p/\rho) - u_j \partial_j u_i + \frac{1}{(\mu\rho)} B_j^{ext} \partial_j b_i + \nu \Delta u_i, \quad (4.1)$$

$$\partial_t b_i = B_j^{ext} \partial_j u_i + \eta \Delta b_i. \quad (4.2)$$

This approximation will be referred to as the *quasi-linear (QL) approximation* since only the non-linear terms involving the magnetic field are discarded whereas the non-linear convective term in the velocity equation is retained. Of course, if $\partial_t b_i$ is neglected in (4.2) one immediately recovers the quasi-static approximation.

4.2. Results

In order to compare the QL approximation with full MHD, we have performed the same numerical simulations as described in section 3, but this time using (4.1) and (4.2) instead of the QS approximation.

4.2.1. Kinetic energy decay

In fig. 5 we present the time history of the kinetic energy (as defined by (3.2)) obtained from both FMHD and the QL approximation. For reference, we have also included the predictions obtained using the QS approximation. For $N = 1$, the QL approximation and FMHD agree nearly perfectly for all values of the magnetic Reynolds number. For $N = 10$, the agreement is still very good.

4.2.2. Magnetic energy evolution

Figure 6 represents the time evolution of the energy of the magnetic fluctuations (defined by (3.3)) for the different runs. For $N = 1$ there is a systematic overestimate of the energy by the QL approximation which (as expected) increases with the magnetic Reynolds number. Contrary to the predictions of the kinetic energy, the performance of the QL approximation is better here when $N = 10$. Even at $R_m = 20$, the agreement between the QL approximation and FMHD is very good.

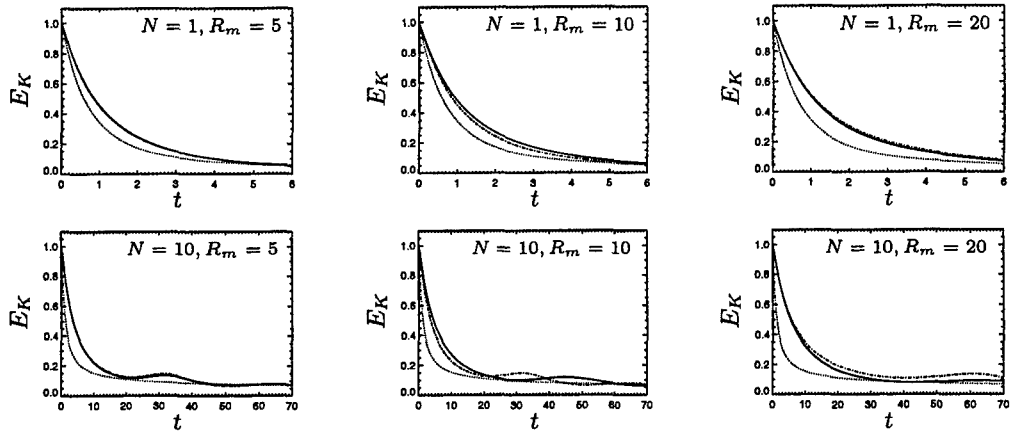


FIGURE 5. Evolution with time of the kinetic energy. — FMHD; - - - QL approximation; QS approximation.

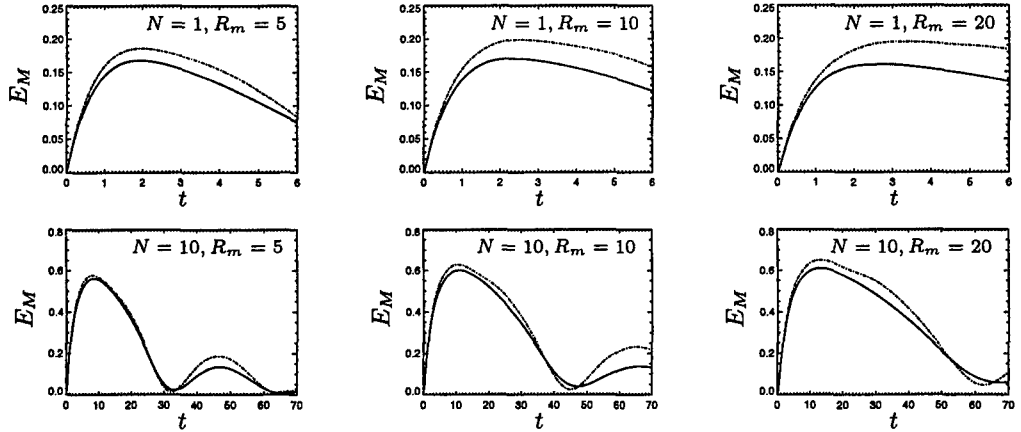


FIGURE 6. Evolution with time of the magnetic energy. — FMHD; - - - QL approximation.

4.2.3. Anisotropy

In fig. 7, the anisotropy angle θ_u computed from the QL approximation and FMHD is displayed. For reference we have also included the anisotropy evolutions predicted using the QS approximation, which as expected are inadequate especially for $R_m = 10$ and $R_m = 20$. In the runs with $N = 1$, the anisotropy predicted by the QL approximation is always more pronounced than for FMHD. For the runs at $N = 10$, the same remark holds for the beginning of the decay. After a certain amount of time, the trend inverses and the anisotropy is more pronounced in the case of FMHD. This appears to be due to a rapid saturation of anisotropy in the QL runs.

The comparison of the anisotropy angles θ_b are presented in fig. 8. Here the trend is given by an underestimate of θ_b by the QL approximation. The discrepancy is somewhat more important for the runs where $N = 1$.

The initial trends observed for both θ_u and θ_b are to be expected. Indeed, it is clear that the additional non-linear terms present in the FMHD equations tend to restore isotropy.

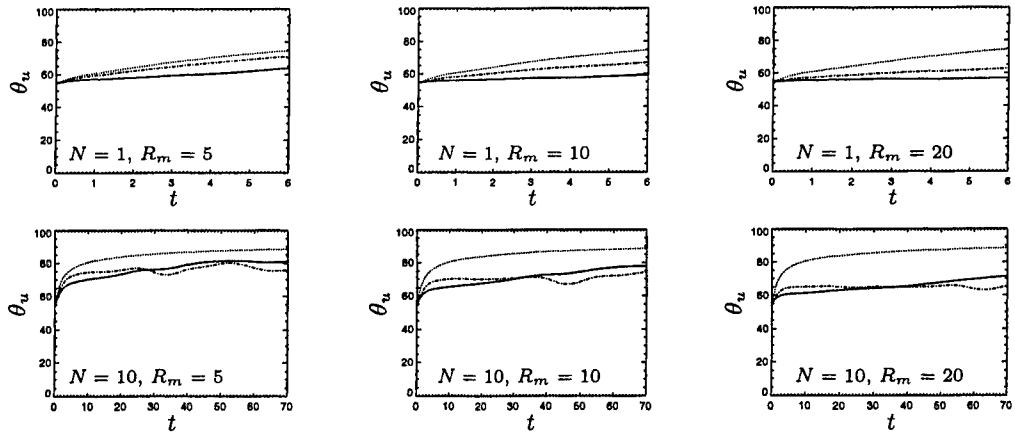


FIGURE 7. Evolution with time of the anisotropy angle θ_u . — FMHD; - - - QL approximation; ····· QS approximation.

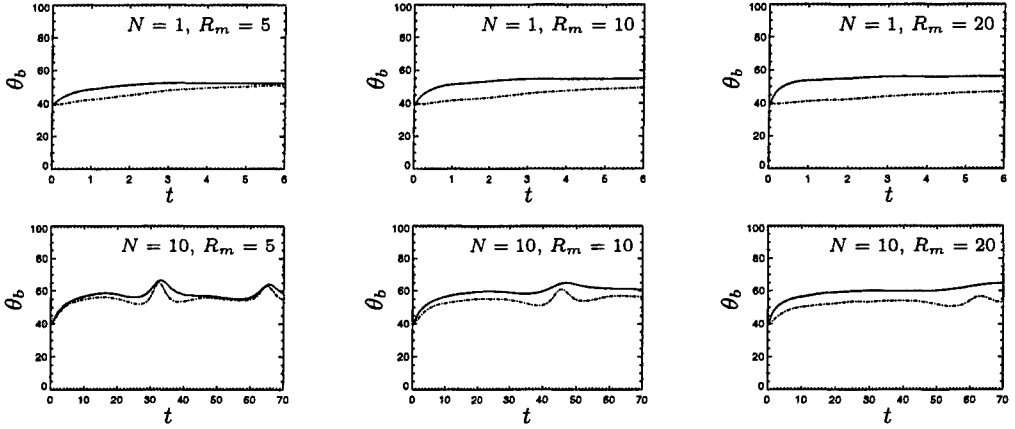


FIGURE 8. Evolution with time of the anisotropy angle θ_b . — FMHD; - - - QL approximation.

This effect will be more pronounced at the beginning of the decay when the flow is more turbulent. In the case of θ_u it is therefore natural to observe an initial overestimate of θ_u by the QL approximation. Similarly, we know from FMHD results discussed earlier that θ_b starts from an initial value of $\simeq 39.2^\circ$ and evolves progressively towards values close to the isotropic value of 54.7° . This trend should be slower in the QL case because of the absence of the non-linear terms and this is exactly what is observed in fig. 8.

5. Conclusions and future plans

The Quasi-Static (QS) approximation offers a valuable engineering approximation for the prediction of MHD flows at small magnetic Reynolds numbers $R_m \ll 1$. However, important technological applications, such as advanced propulsion and flow control schemes for hypersonic vehicles, involve MHD and MGD flows at moderate magnetic Reynolds numbers $1 \lesssim R_m \lesssim 20$. In order to devise successful schemes for the prediction of these technological flows we need to understand better the intermediate regime that bridges

the domain where the QS approximation is valid and the high- R_m regime, where full nonlinear MHD (FMHD) is the only resort.

By studying the case of decaying homogeneous MHD turbulence, we have established that the Quasi-Static (QS) approximation is valid for $R_m \lesssim 1$, but progressively deteriorates as R_m is increased beyond 1. The magnetic Stuart number does not seem to have a strong effect on the accuracy of the QS approximation. That is, at a given R_m , the accuracy of the QS approximation is roughly the same for $N = 1$ as it is for $N = 10$.

We have studied another approximation, the QL approximation, for use at higher R_m . As with the QS approximation, this approximation assumes small magnetic fluctuations, but it resolves the time dependence of these fluctuations explicitly. The QL approximation, as we expected when we proposed it, performs like the QS approximation for $R_m \lesssim 1$, but has the advantage that it retains good agreement with FMHD for $1 \lesssim R_m \lesssim 20$. It should be noted that $R_m = 20$ is the highest value of the magnetic Reynolds number that we have tested during this effort. Therefore, our numerical simulations indicate that the QL approximation should be adopted in place of the QS approximation for flows with a moderate value of the magnetic Reynolds number ($0 \lesssim R_m \lesssim 20$).

We are currently engaged in the development of structure-based closures of the QL approximation for homogeneous turbulence in a conductive fluid subject to mean deformation and a uniform external magnetic field. This effort builds on earlier work that dealt with the modeling of decaying homogeneous MHD turbulence.

Acknowledgements

The authors are grateful G. Burton for his comments on this manuscript and to the Center for Turbulence Research for hosting and providing financial support for part of this work during the 2002 Summer Program. S.K. wishes to acknowledge partial support of this work by AFOSR. B.K. and D.C. are researchers of the Fonds National pour la Recherche Scientifique (Belgium). This work has also been supported in part by the Communauté Française de Belgique (ARC 02/07-283) and by the contract of association EURATOM - Belgian state. The content of the publication is the sole responsibility of the authors and it does not necessarily represent the views of the Commission or its services.

REFERENCES

DAVIDSON, P. 2001 *An Introduction to Magnetohydrodynamics*. Cambridge University Press.

DAVIDSON, P. A. 1995 Magnetic damping of jets and vortices. *J. Fluid Mech.* **299**, 153–186.

HOSSAIN, M. 1991 Inverse energy cascades in three dimensional turbulence. *Phys. Fluids B* **3** (3), 511–514.

KASSINOS, S. C. & REYNOLDS, W. C. 1994 A structure-based model for the rapid distortion of homogeneous turbulence. *Tech. Rep. TF-61*. Mechanical Engineering Dept.

KASSINOS, S. C. & REYNOLDS, W. C. 1999 Structure-based modeling for homogeneous MHD turbulence. In *Annual Research Briefs 1999*, pp. 301–315. Stanford University and NASA Ames Research Center: Center for Turbulence Research.

KASSINOS, S. C., REYNOLDS, W. C. & ROGERS, M. M. 2001 One-point turbulence structure tensors. *J. Fluid Mech.* **428**, 213–248.

LEHNERT, B. 1955 The decay of magneto-turbulence in the presence of a magnetic field and coriolis force. *Quart. Appl. Math.* **12** (4), 321–341.

LUMLEY, J. L. 1978 Computational modeling of turbulent flows. *Ad. Appl. Mech.* **18**, 123.

MOFFATT, H. K. 1967 On the suppression of turbulence by a uniform magnetic field. *J. Fluid Mech.* **28**, 571–592.

OUGHTON, S., PRIEST, E. & MATTHAEUS, W. 1994 The influence of a mean magnetic field on three-dimensional magnetohydrodynamic turbulence. *J. Fluid Mech.* **280**, 95.

REYNOLDS, W. C. & KASSINOS, S. C. 1995 One-point turbulence structure tensors. *Proc. Royal Society London A* **451**, 87–104.

ROBERTS, P. H. 1967 *An Introduction to Magnetohydrodynamics*. American Elsevier Publishing Company, Inc. New York.

SCHUMANN, U. 1976 Numerical simulation of the transition from three- to two-dimensional turbulence under a uniform magnetic field. *J. Fluid Mech.* **74**, 31–58.

SHEBALIN, J. V., MATTHAEUS, W. H. & MONTGOMERY, D. 1983 Anisotropy in MHD turbulence due to a mean magnetic field. *J. Plasma Phys.* **29** (3), 525–547.

SOMMERIA, J. & MOREAU, R. 1982 Why, how, and when, MHD turbulence becomes two-dimensional. *J. Fluid Mech.* **118**, 507–518.

ZIKANOV, O. & THESS, A. 1998 Direct numerical simulation of forced MHD turbulence at low magnetic Reynolds number. *J. Fluid Mech.* **358**, 299–233.